Compliant electrodes based on platinum salt reduction in a urethane matrix

View the article online for updates and enhancements.

Compliant electrodes based on platinum salt reduction in a urethane matrix

Remi Delille, Mario Urdaneta, Kuangwen Hsieh and Elisabeth Smela[1]

Mechanical Engineering Department, University of Maryland, College Park, MD 20742, USA

E-mail: smela@eng.umd.edu

Abstract
An elastomeric but electrically conducting material is presented that is
fabricated using a method inspired by ionic polymer–metal composites. The
Young's modulus is only 10 MPa, and yet the conductivity is nearly 1 S cm^{-1}
and the material remains electrically conductive under uniaxial strains of
30%. Furthermore, this electrode material is photopatternable. Fabrication
begins with mixing the platinum salt tetraammineplatinum(II) chloride into a
UV-curable acrylated urethane elastomer precursor (Loctite 3108). The
mixture is crosslinked under UV light in less than a minute and can therefore
be patterned if it is exposed through a mask. The salt is then chemically
reduced with sodium borohydride, which results in the formation of 100 nm
sized platinum nodules on the surface of the film.

1. Introduction

Materials that are electrically conductive but mechanically
compliant are needed in a wide range of applications, from
artificial tactile skins [1] (for example, for robotics and
prosthetics) to smart textiles [2] and artificial muscles [3].
The electrical conductivities that are required range from
low (10^{-10}–10^{-7} S cm^{-1}) for applications such as discharge
protection [4], to medium (10^{-3}–10^{1} S cm^{-1}) for strain
gauges [5] and for electrodes used in dielectric elastomer
actuators (DEAs) [6, 7] and capacitive sensors [8], to high
($>10^{1}$ S cm^{-1}) for electrical interconnects and stretchable
electronics [9] with low power consumption, low resistive
heating, and fast response times.

The goal of this research was to produce a robust,
elastomeric, high conductivity material that could be patterned
using standard microfabrication methods. These compliant
electrodes were expected to survive handling and use in actual
applications without damage. For use in devices such as DEAs
and smart textiles, the electrodes must be able to stretch tens of
per cent or more, without breaking or losing conductivity, and
return to their original length when the stresses are removed.
High conductivity was a goal because if it could be achieved,
then it would be straightforward to dial the conductivity down
as needed. For any microscale component or device, or any

that interface between the meso- and microscales, including
many of the applications given above, micro-patternability of
the electrodes is required. The most preferable is if the material
can be photopatterned, because this is a one-step, low-cost
method that can be performed on large, nonplanar surfaces, as
well as small, flat ones, and it thus provides flexibility in the
manufacturing process and for system integration. In addition,
the research aimed to produce a material that could sustain high
strain rates without damage.

Compliant electrodes are already available, but none
display all of the characteristics previously described. Thus,
the development of a novel material could extend the
capabilities of existing devices as well as enable new
technologies. There are four existing types of compliant
electrodes: conducting-particle-loaded polymers, thin metal
films on polymer substrates, carbon grease or graphite powder,
and electrostatically assembled materials. Loading metallic
particles into a polymer is simple and common, but while
particle-loaded elastomers can reach reasonable conductivities,
the Young's modulus climbs orders of magnitude with loading,
so the materials are no longer elastomeric [10, 11]. While
photopatterning is possible using this approach, the particles
(metals, carbon black or carbon nanotubes, even inherently
conducting polymers) strongly interfere with the process due
to light absorption or scattering [11, 12]. High strains and
conductivities can be obtained by coating elastomers with thin
metal films [13], and the achievable strain can reach 50–100%

---

[1] Author to whom any correspondence should be addressed.

if the film is corrugated out of plane (e.g. by stretching the substrate during deposition [7, 9, 14]) or if it is sinusoidally shaped in the plane [15, 16], but this approach suffers from delamination at the polymer–metal interface, especially at defects [13, 17]. Although metal films on elastomer substrates have been patterned using microfabrication methods such as lift-off [18], patterning can be challenging, particularly in cases where the photolithography steps cause elastomer swelling or adverse chemical reactions, and pre-stretching is incompatible with microfabrication. Carbon grease [6, 19, 20] and graphite powder [21–23] are currently used in dielectric elastomer actuators and allow impressive areal strains of more than 300%. Unfortunately, they can rub or wear off, and they cannot be integrated into microfabricated devices. Layer-by-layer electrostatic self-assembly incorporating metal nanoparticles produces excellent robustness, elasticity (hundreds of per cent strain), and conductivity [24], but the resulting materials are very expensive, and methods for integration with microfabrication techniques are unclear (they are produced in the form of free-standing sheets).

This paper introduces a new fabrication method to form robust, conductive, photopatternable elastomers. The approach was inspired by the electrode formation process used in ionic polymer–metal composites (IPMCs) [25–28].

2. Experimental details

2.1. Fabrication of composite films

Films were fabricated using the elastomer Loctite 3108 (Henkel), the metal salt tetraammineplatinum(II) chloride (Sigma-Aldrich), and the reducing agent sodium borohydride (Sigma-Aldrich). Loctite 3108 is an acrylated urethane with a proprietary structure. The fabrication procedure consisted of three steps: mixing the salt into the elastomer precursor, exposing the mixture to ultraviolet light to form the elastomer and pattern the electrode shape, and chemically reducing the salt to metal in the borohydride solution.

The tetraammineplatinum(II) chloride (2.74 g cm^{-3}) was ground with a mortar and pestle for 5 min. It was added into the 3108 elastomer precursor (1.08 g cm^{-3} [29]) in concentrations varying from 0 to 15 vol% and hand-mixed for 20 min, followed by homogenization at 10 000 rpm for 2 min (T18 Ultra Turrax homogenizer). Air bubbles in the mixture were removed in a benchtop vacuum chamber (10 Torr, 5 h).

Loctite 3108 is an adhesive, but it does not stick to SealView, a transparent polyolefin film (Norton Performance Plastics). The 3108/salt mixture was sandwiched between glass slides protected with SealView. Spacers were used to define a film thickness between 100 and 150 μm [29]. The front and back sides of the film were exposed to a dose of 100 mJ cm^{-2} UV light (Spectroline EN-180, center wavelength 365 nm, power flux of 5 mW cm^{-2} [29], 20 s on each side). The film was peeled from the SealView and cut into rectangular samples (25 mm × 15 mm × 150 μm for conductivity measurements and 35 mm × 3 mm × 100 μm for Young's modulus and resistance versus strain measurements).

To chemically reduce the platinum salt, the films were immersed in an aqueous 30 mM solution of sodium borohydride (Sigma-Aldrich) at 60 °C for 5 h. The reduction step was repeated one time.
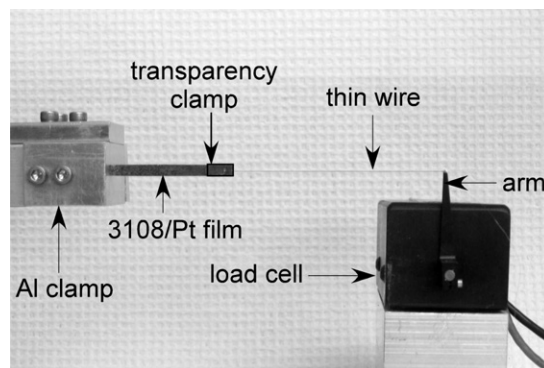

Figure 1. Set-up for Young's modulus measurement.

2.2. Conductivity measurement

Conductivity was measured using the four-point-probe technique [30] with four 0.64 mm diameter wires spaced 2.75 mm apart. A digital multimeter (Fluke 8505A) supplied the current to the outer pair of electrodes and also measured the voltage drop across the two inner electrodes. The geometric correction factor G for thin rectangular samples was used to determine the resistivity ρ:

$$\rho = G \times R = \frac{\pi}{\ln(2)} \times t \times R_1\left(\frac{b}{s}, \frac{a}{b}\right) \times R \qquad (1)$$

where t is the film thickness, a the film width, b the film length, s the probe spacing, and R the resistance [31]. The function R_1 is tabulated for various geometries in [31][2]. Since the electrical conductivity was tabulated using the thickness of the entire film, it is appreciably lower than that calculated from the thickness of just the metallized surface layer.

2.3. Young's modulus measurement

The Young's modulus was measured using a force–strain transducer (Model 300B, Aurora Scientific) [32]. Custom LabView software controlled the arm on the transducer head to provide a strain rate of 0.67% s^{-1}, and it also monitored the force. The Young's modulus was obtained from the slope in the region from 0.5 to 2.0% elongation on the stress–strain curve.

Figure 1 displays the experimental test set-up. Since the composite films are soft, the sample was rigidly clamped at both ends to avoid tearing. Two aluminum blocks served as a clamp at one end, and two 3 mm × 5 mm transparency strips glued to both lateral faces of the film served as the other clamp. Loctite 4304 was used to adhere the transparency clamps to the composite samples. The use of 4304 minimized slip since it is 100 times stiffer, at a Young's modulus of 1.6 GPa [33], than 3108. A 500 μm diameter through-hole was drilled in the center of the transparency clamp, and 0.002 inch diameter wire (California Fine Wire Company) was passed through the hole and tied to the arm of the tensile tester.

---

[2] With the correction factor, the calculated electrical resistivity was 25% higher than that calculated from $\rho = RA/l$, where A and l are the cross-sectional area and length of the sample, respectively.

2.4. Scanning electron microscopy

Scanning electron micrographs were taken with an AMRAY 1820D at 20 kV. Energy dispersive (x-ray) spectrometry (EDS) was also performed on a 12 vol% 3108/Pt sample with an EDAX DX-4 x-ray microanalysis system. Samples were cryogenically freeze-fractured to obtain cross-sectional images.

2.5. Resistance versus strain measurements

For resistance versus strain measurements, the samples were mounted in an Instron 8841 tensile tester (2 kN Dynacell load cell) with aluminum clamps. They were elongated at 0.2% s^{-1}. The resistance was measured using a two-point-probe technique in which a voltage supply (Lambda LPD-422A-FM) applied 5.04 V across a 10 kΩ resistor in series with the 3108 composite film. A 1.48 MΩ resistor was used when the resistance of the sample surpassed 40 kΩ. During uniaxial loading, a LabView data acquisition program monitored the voltage drop across the sample. The 2 kN load cell had ±0.25% repeatability for a force range of 20–2000 kN. Due to the size and softness of the composites, the force on the composite samples was always less than 2 N. The resolution was thus unknown in this range, and force data could not be extracted from these measurements.

3. Results and discussion

3.1. Composite formation

The salt had a large distribution in the sizes of the crystallites, from below 1 μm to a maximum of ∼100 μm. The crystals did not dissolve appreciably when mixed into the Loctite 3108, or during curing.

The exposure time needed to crosslink the 3108 was determined in previous work [29] and was unaffected by salt loading. This is in contrast to conducting nanoparticles, which absorb or scatter light, as mentioned above. This route to the formation of conductive elastomers is therefore unique in completely preserving photopatternability, and relies on the fact that the metal salt is transparent, unlike the metal.

Upon reduction, the material became gray, opaque, and shiny [11]. Some of the platinum precipitated in the reduction solution and not in or on the polymer, seen as an increasing gray cloudiness of the solution over time. The amount of reduced platinum in the composites is thus unknown.

The metal formed primarily on the surface, as shown in figure 2. The SEM images show that the platinum (bright regions) precipitated into nodules approximately 100 nm in diameter on the elastomer surface (dark). Energy dispersive spectroscopy (EDS) confirmed that these nodules were Pt. EDS detected no Cl or N anywhere in the composite, showing that all the ions had left the polymer.

The adhesion of the metal to the elastomer was tested using a standard tape test (Scotch Magic, 3M). This is a threshold test: it determines whether the metal adheres more strongly to the elastomer or to the tape. Since the composites were more elastic than the tape, this resulted in a strain of ∼80% when the tape was peeled off, which added further stress. Only dustings of metal were removed by the tape,
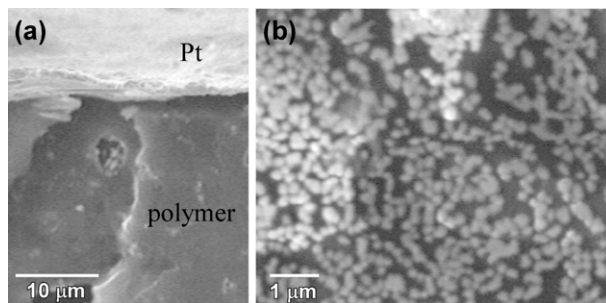

Figure 2. (a) Cross-sectional view of a sample loaded with 11 vol% salt prior to reduction. (b) Overhead view of the surface of a sample loaded with 7 vol% salt prior to reduction.

even when the test was applied multiple times to the same sample. The amount of dust that came off increased with the salt loading, but the metal adhered better to the sample in all cases (i.e. the appearance of the composites did not change following the tests).

Water swells Loctite 3108 by 10% [29], but the fact that the Pt was only on the surface, and that there were no ions left in the polymer, suggests that the sodium borohydride did not appreciably penetrate into the polymer, and that the reaction occurred when the salt diffused into the polymer surface. The nodules indicate a nucleation process. This implies that the ionic species have a quite small partition coefficient (the ratio of the concentration of salt in the polymer to that in the water at equilibrium), which is not unexpected for charged species in a hydrophobic matrix.

3.2. Conductivity versus salt loading

When a host matrix is loaded with a conducting material, the conductivity typically increases sharply at the percolation threshold, the loading at which the particles become sufficiently interconnected to provide electrical conduits across the material [10, 34–36]. To map the conductivity versus loading curve for the 3108/Pt composites, samples were prepared with salt concentrations from 0 to 15 vol%. It is important to note that the results are presented with respect to salt loading concentration, which does not represent the amount of conducting platinum in the composite.

As illustrated in figure 3, below 5 vol% (region I), the conductivity of the composites was too small to register on the multimeter, which had an upper limit of 2.65×10^8 Ω ($>4 \times 10^{-6}$ S cm^{-1}). The conductivity became measurable at a salt concentration of 5 vol%, and in region II, the percolation regime, increased approximately one order of magnitude with each additional 1 vol% (from 10^{-4} to 0.5 S cm^{-1}). Based on percolation theory, the relationship between concentration and conductivity should follow a power law. The solid line in figure 3 is a power law fit to the data within the percolation regime. Above 10 vol%, the electrical conductivity remained constant.

Interpreting the data based on percolation theory, platinum particles produced by the reduction process should be sufficiently isolated from each other in region I that they do not form long conducting paths across the sample [10]. Figure 4(a) shows the surface of a sample at 5 vol%, the point at which electrical conduction just became measurable. Some
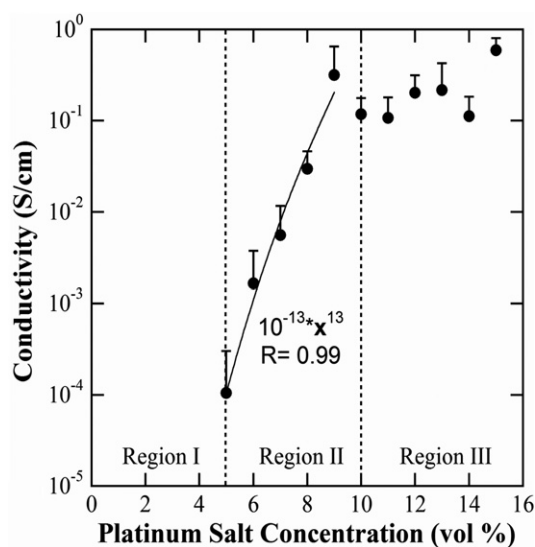
Figure 3. Percolation curve for the 3108/Pt films (semi-logarithmic scale). The error bars show the standard deviations, based on three measurements each on at least four samples (negative error bars not shown), and the line is a power law fit.

particle interconnection is visible, consistent with the electrical measurements. The distribution of platinum on these samples is strikingly similar to that reported by Nemat-Nasser *et al* for Flemion-based IPMCs [28].

Figure 4(b) shows the surface of a 10 vol% sample, at the upper end of the percolation regime, on which large spanning clusters are visible and individual platinum nodules are difficult to discern. The large error bars in figure 3 reflect the inhomogeneous distribution of metal. At a loading of 15 vol%, figure 4(c), the Pt homogeneously covered the entire surface, consistent with the data in figure 3 showing that these samples have the highest conductivity and smallest variation between samples.

The variations in conductivity are not critical for technologies that operate at high voltage and low current, such as DEAs, but for other applications this may be unacceptable. Techniques have been developed for IPMCs to increase platinum homogeneity, such as introducing dispersing agents during the reduction process [26, 27], and these may be applicable to the 3108/Pt composites. Another technique used in IPMCs is electroplating a layer of gold or platinum to enhance interconnection between the particles [26, 27, 37].

This was done on a 12 vol% 3108/Pt sample, giving an increase in conductivity from 0.2 to 12 S cm^{-1}, but a 40% drop in maximum strain before electrical failure. This method is therefore inappropriate for elastomeric conductors. Varying parameters during the manufacturing procedure, such as temperature [26], solution concentration [26, 38], immersion time [38], or homogenization conditions [36], has been shown to improve the spatial distribution of the metal in polymer–metal composites. More specifically, increasing the mixing time and temperature improved homogeneity in carbon black [36] and polyaniline [39] loaded composites.

3.3. Young's modulus

The key goal of this research was to produce a conductive material that remained elastomeric. The Young's modulus at each loading was therefore measured. The stress–strain curve for a 14 vol% composite is shown in figure 5(a). The slope of the curve changed over the strain range, as is typical of most polymers [40]. We arbitrarily chose 0.5–2.0% strain as the interval from which to estimate the moduli, and these are plotted in figure 5(b). Each point represents the average of 10 measurements each on at least four samples. One standard deviation error bars, not shown, are approximately the same size as the symbols in the figure.

The modulus of unloaded 3108 was 9 MPa. As the platinum salt concentration increased, the modulus, surprisingly, decreased. The interaction between the platinum particles and matrix is not a mechanically reinforcing one, as observed in most particle-loaded composites [40].

Voids are known to decrease the modulus [40]. Small platinum salt crystals were present in the mixture prior to UV exposure, and the polymer must form around them. We hypothesize that nano- to microscale voids were thereby produced during the reduction step when the salt diffused out of the polymer. These small voids would be difficult to observe in SEM images of sample cross sections. In the more highly loaded samples, tens of μm-sized macro-voids were observed (figure 6), which may account for the large drop in modulus in region III (10–15% loading).

3.4. Resistance under uniaxial strain

Compliant electrodes must remain conductive under strain, and preferably experience minimal hysteresis. The resistance under uniaxial strain was measured for samples above the
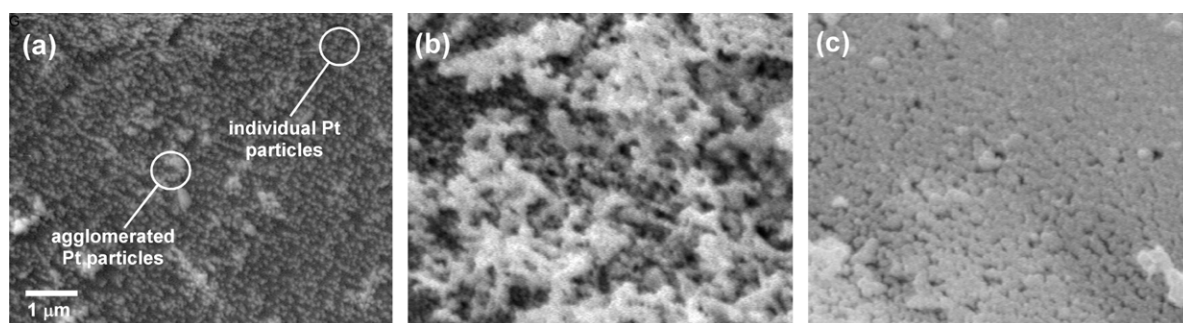

Figure 4. Scanning electron micrographs of 3108/Pt composite surfaces with (a) 5 vol%, (b) 10 vol% and (c) 15 vol% platinum salt loading at 15 kV. (All micrographs are at the same magnification.)
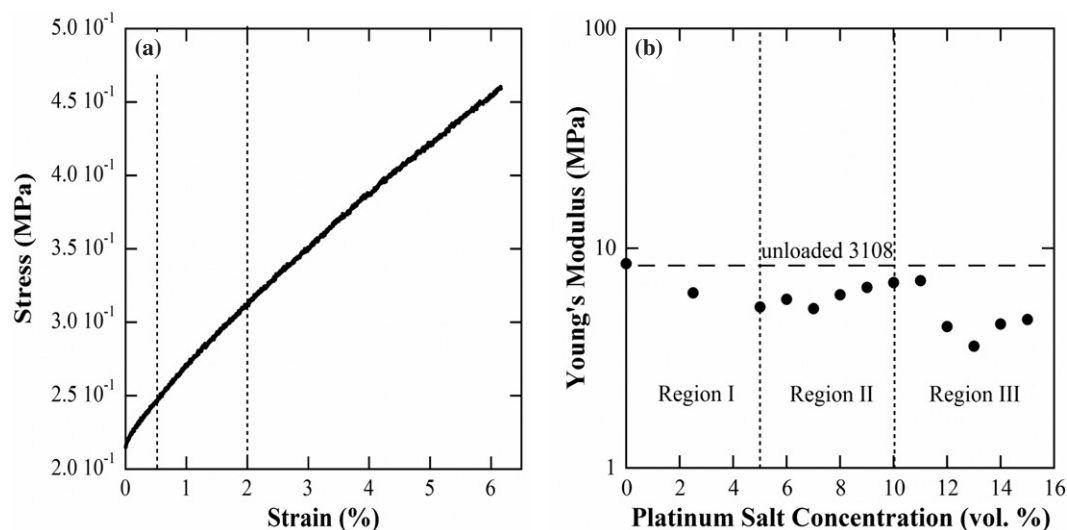
Figure 5. (a) Stress–strain curve for a 14 vol% 3108/Pt sample. The Young's modulus was obtained from the slope between 0.5 and 2.0% strain. (b) Young's modulus with respect to platinum salt loading (semi-logarithmic scale).
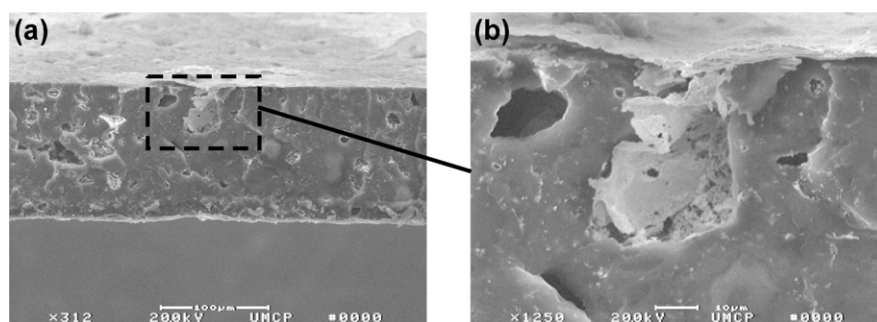

Figure 6. (a) Micrograph of cross section of a 3108/Pt composite film formed with 11 vol% salt concentration. (b) Close-up shows a macro-void filled with Pt and two smaller macro-voids.
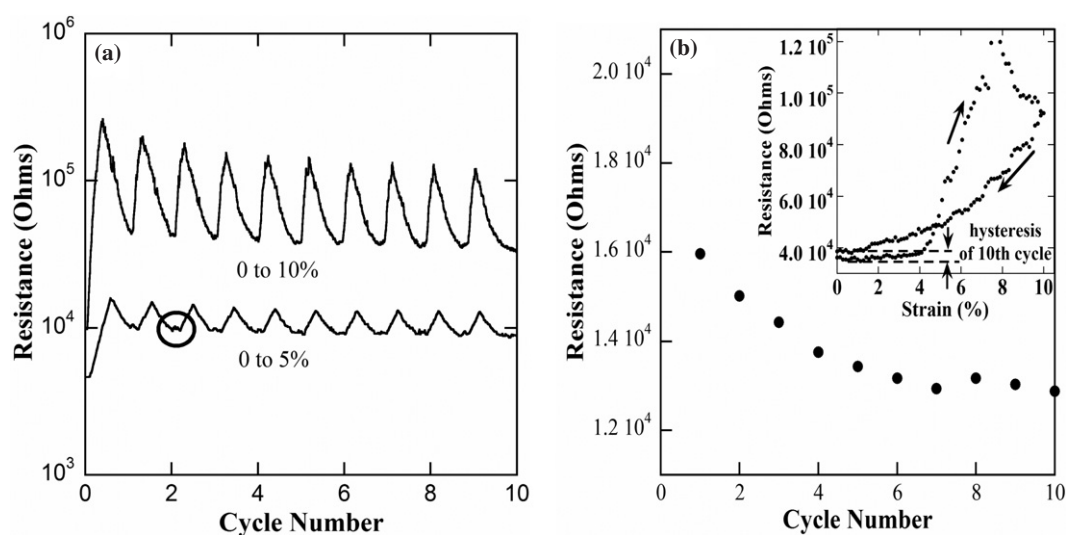

Figure 7. (a) Resistance of a 14 vol% 3108/Pt composite during strain cycling from 0 to 5 and 0 to 10% elongation (semi-logarithmic scale). (b) Maximum resistance during strain cycling to 5%, where the inset is a resistance–strain hysteresis loop for the tenth cycle from 0 to 10% strain.
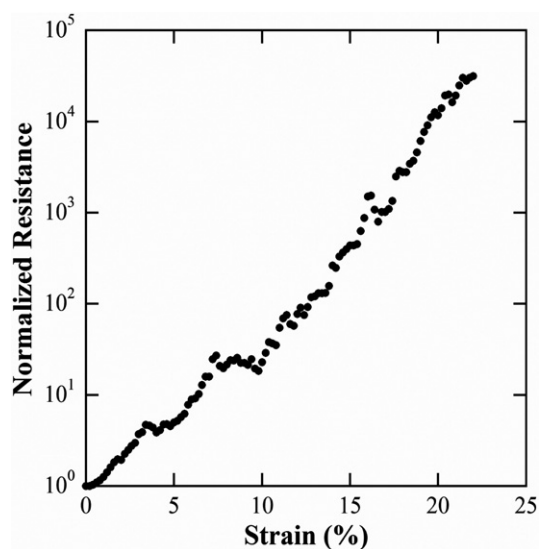
Figure 8. Strain to electrical failure at a strain rate of 0.2% s^{-1} for a 14 vol% composite (semi-logarithmic scale). The normalized resistance is R/R_0, where R is the resistance at the specific strain value and R_0 is the initial resistance.

percolation threshold (14 vol%). Since viscoelastic effects are minimized at low strain rates [41], the samples were elongated at 0.2% s^{-1}.

Figure 7(a) shows the resistance of a sample cycled ten times from 0 to 5% strain followed by 10 cycles from 0 to 7.5% (not shown) and 0 to 10%. The resistance was approximately linear with strain. It increased irreversibly during the first cycle to 5% (from 4.6 to a maximum of 16 kΩ), and again during the first cycle to 10% (from 9.8 to a maximum of 250 kΩ), marking a significant electrical hysteresis or unrecoverable electrical conductivity due to the Mullins effect [30]. During subsequent cycles, the maximum resistance dropped somewhat, stabilizing at 13 kΩ for the 5% strain cycles (figure 7(b)). Following the ten cycles to 5 and 10%, the electrical resistance in the relaxed state recovered to 8.7 and 23.5 kΩ, for a net resistance increase of 89% and 140%, respectively.

During relaxation from 5% back to 0% elongation, the arms of the tensile tester moved together faster than the film contracted, marked by the circled region in figure 7(a), so that the films buckled. This mechanical hysteresis was less pronounced during the subsequent cycles to 10% elongation. Slow relaxation has been observed in other particle-loaded composites and was attributed to stress softening [30].

The samples were also strained to electrical failure (figure 8). The resistance increased approximately exponentially with strain up to 26.5%, at which point it suddenly jumped beyond the detection limit of the experimental set-up; this was defined as electrical failure. (This is not the same as the ultimate strain, which is the point at which the material ruptured mechanically.) The samples recovered their conductivity when the strain was reduced. Applying the percolation model, electrical failure occurred when the platinum nodules become sufficiently separated so as to break all electrical paths across the sample.

Since this material is being explored as a compliant electrode for applications such as dielectric elastomers, it is necessary to know its mechanical integrity under high strain rates. Composite samples at 5, 9, and 13 vol% loading were cycled 10 times each at a strain rate of 6.7% s^{-1} to 13% strain and then examined using SEM. In the 5 and 9 vol% samples, the high strain rates created micro-cracks (<1 μm in width and 5 μm in length), a phenomenon also observed on the surfaces of IPMC transducers [27]. In the 13 vol% sample, the platinum wrinkled (figure 9). The images suggest that either the platinum may not be not strongly bound to the polymer and partially delaminated from it, or that the composite plastically deformed and formed wrinkles upon relaxation. Given that cracks and wrinkles do not interfere with electrode performance in IPMCs and thin metal films on elastomers, they are unlikely to interfere with the conductivity or modulus of these composites, but this requires further study.

4. Conclusions

A novel compliant electrode fabrication method has been presented that offers several advantages over existing methods. The fact that the metal is initially put into the material as a transparent salt allows the elastomer to be photo-cured, which means that the electrodes can readily be patterned into any desired shape and integrated with microfabricated components. The formation of a metal skin on the surface of the polymer that is made up of small nodules keeps the modulus of the composite low. Since the metal is formed as it emerges from the polymer during the reduction process, it adheres
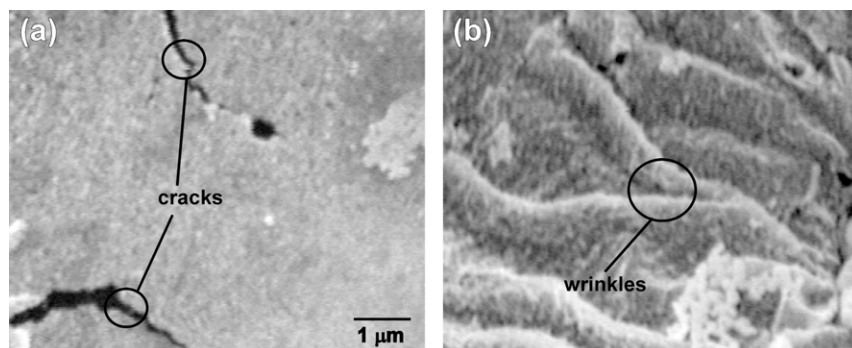

Figure 9. SEM micrograph of sample surfaces exhibiting (a) micro-cracks and (b) wrinkles after 10 cycles at high strain rate (6.7% s^{-1}). (Magnification is the same in these images.)

well, and the material can thus readily withstand strains of tens of per cent without significant loss in performance. The conductivity, after an initial 'break-in', is not lost with strain cycling at low strain rates, although this must still be shown at higher strain rates.

The Pt-coated elastomers, while promising, are not yet ideal, however: maximum strains and strain rates, hysteresis and mechanical lag, and cost should all be improved. The fabrication method has not been optimized in any way, and there is every reason to expect that there can be significant improvements in performance by adjusting the numerous process parameters. Furthermore, the use of other metal salts, such as silver nitrate or copper sulfate, could substantially reduce the cost.

The performance of these conductive elastomers is already sufficient for low and medium conductivity applications. The composites in region I have a conductivity below 10^{-4} S cm^{-1}, but the upper end of this region is useful for low-current applications, for which conductivities as low as 10^{-10} S cm^{-1} are acceptable. In addition, for films in regions II and III, the conductivity, and the essentially linear change in conductivity, make these materials of use as strain gauges. The goals set out at the beginning of the paper were therefore substantially met. However, the performance is not yet sufficient for the highest conductivity applications or for dielectric elastomer actuators. The modulus is acceptable, but additional research is required to produce materials that can undergo hundreds of per cent strain at extremely high strain rates for millions of cycles.

Acknowledgments

References

[1] Ko W 1996 The future of sensor and actuator systems *Sensors Actuators* A **56** 193–7
[2] Service R F 2003 Electronic textiles charge ahead *Science* **301** 909–11
[3] Ashley S 2003 Artificial muscles *Sci. Am.* **289** 52–9
[4] Tsotra P and Friedrich K 2002 Electrical and mechanical properties characterization of epoxy resin/polyaniline-dodecylbenzenesulphonic acid salt composite materials *J. Polym. Mater.* **19** 389–94
[5] Schnack E, Prinz B and Dimitrov S 2004 Interlaminar stress determination in carbon fibre epoxy composites with the embedded strain gauge technique *Strain* **40** 113–8
[6] Pelrine R, Kornbluh R, Pei Q B and Joseph J 2000 High-speed electrically actuated elastomers with strain greater than 100% *Science* **287** 836–9
[7] Watanabe M, Shirai H and Hirai T 2002 Wrinkled polypyrrole electrode for electroactive polymer actuators *J. Appl. Phys.* **92** 4631–7
[8] Engel J M, Chen N, Ryu K, Pandya S, Tucker C, Yang Y and Liu C 2006 Multi-layer embedment of conductive and non-conductive PDMS for all-elastomer MEMS *Solid State Sensors, Actuators, and Microsystems Workshop (Hilton Head, SC, June 2006)* pp 316–9
[9] Jones J, Lacour S P, Wagner S and Suo Z G 2004 Stretchable wavy metal interconnects *J. Vac. Sci. Technol.* A **22** 1723–5
[10] Sau K P, Chaki T K and Khastgir D 1998 Carbon fibre filled conductive composites based on nitrile rubber (NBR), ethylene propylene diene rubber (EPDM) and their blend *Polymer* **39** 6461–71
[11] Delille R, Urdaneta M, Hsieh K and Smela E 2006 Novel compliant electrodes based on platinum salt reduction *EAPAD: Proc. 13th Int. Symp. Smart Struc. Mater., Electroactive Polymer Actuators and Devices (San Diego, CA, Feb.–March 2006)*; *Proc. SPIE* at press
[12] Jiguet S, Bertsch A, Hofmann H and Renaud P 2005 Conductive SU8 photoresist for microfabrication *Adv. Funct. Mater.* **15** 1511–6
[13] Li T, Huang Z Y, Xi Z C, Lacour S P, Wagner S and Suo Z 2005 Delocalizing strain in a thin metal film on a polymer substrate *Mech. Mater.* **37** 261–73
[14] Lacour S P, Wagner S, Huang Z Y and Suo Z 2003 Stretchable gold conductors on elastomeric substrates *Appl. Phys. Lett.* **82** 2404–6
[15] Gray D S, Tien J and Chen C S 2004 High-conductivity elastomeric electronics *Adv. Mater.* **16** 393–7
[16] Pelrine R, Kornbluh R, Joseph J, Heydt R, Pei Q B and Chiba S 2000 High-field deformation of elastomeric dielectrics for actuators *Mater. Sci. Eng.* C **11** 89–100
[17] Li T, Huang Z Y, Suo Z, Lacour S P and Wagner S 2004 Stretchability of thin metal films on elastomer substrates *Appl. Phys. Lett.* **85** 3435–7
[18] Lacour S P, Tsay C and Wagner S 2004 An elastically stretchable TFT circuit *IEEE Electron. Device Lett.* **25** 792–4
[19] Kofod G, Sommer-Larsen P, Kornbluh R and Pelrine R 2003 Actuation response of polyacrylate dielectric elastomers *J. Intell. Mater. Syst. Struct.* **14** 787–93
[20] Pope K, Tews A, Frecker M I, Mockenstrum E, Goulbourne N and Snyder A J 2004 Dielectric elastomer laminates for active membrane pump applications *EAPAD: Proc. 11th Int. Symp. Smart Struc. Mater., Electroactive Polymer Actuators and Devices (San Diego, CA, March 2004)*; *Proc. SPIE* **5385** 60–7
[21] Heydt R, Pelrine R, Joseph J, Eckerle J and Kornbluh R 2000 Acoustical performance of an electrostrictive polymer film loudspeaker *J. Acoust. Soc. Am.* **107** 833–9
[22] Heydt R, Kornbluh R, Pelrine R and Mason V 1998 Design and performance of an electrostrictive-polymer-film acoustic actuator *J. Sound Vib.* **215** 297–311
[23] Pelrine R E, Kornbluh R D and Joseph J P 1998 Electrostriction of polymer dielectrics with compliant electrodes as a means of actuation *Sensors Actuators* A **64** 77–85
[24] Nanosonic 2006 Material properties sheet, metal rubber http://www.nanosonic.com/MR-01-sheets_productdatasheet.pdf
[25] Onishi K, Sewa S, Asaka K, Fujiwara N and Oguro K 2000 Morphology of electrodes and bending response of the polymer electrolyte actuator *Electrochim. Acta* **46** 737–43
[26] Shahinpoor M and Kim K J 2001 Ionic polymer–metal composites: I. Fundamentals *Smart Mater. Struct.* **10** 819–33
[27] Kim K J and Shahinpoor M 2003 Ionic polymer–metal composites: II. Manufacturing techniques *Smart Mater. Struct.* **12** 65–79
[28] Nemat-Nasser S and Wu Y X 2003 Comparative experimental study of ionic polymer–metal composites with different backbone ionomers and in various cation forms *J. Appl. Phys.* **93** 5255–67

[29] Delille R, Urdaneta M, Moseley S and Smela E 2006 Benchtop polymer MEMS *J. Microelectromech. Syst.* at press

[30] Yamaguchi K, Busfield J J C and Thomas A G 2003 Electrical and mechanical behavior of filled elastomers. I. The effect of strain *J. Polym. Sci.* B **41** 2079–89

[31] Topsoe H 1968 *Geometric Factors in Four Point Resistivity Measurement*

[32] Smela E and Mattes B R 2005 Polyaniline actuators, part 2: PANI(AMPS) in methanesulfonic acid *Synth. Met.* **151** 43–8

[33] Loctite 2005 Technical data sheet, Loctite 4304

[34] Jiguet S, Bertsch A, Hofmann H and Renaud P 2004 Conductive SU8-silver composite photopolymer *17th IEEE Int. Conf. on Micro Electro Mechanical Systems (Maastricht, Jan. 2004)* (Piscataway, NJ: IEEE) pp 125–8

[35] Gubbels F, Jerome R, Teyssie P, Vanlathem E, Deltour R, Calderone A, Parente V and Bredas J L 1994 Selective localization of carbon black in immiscible polymer blends:

a useful tool to design electrical conductive composites *Macromolecules* **27** 1972–4

[36] Gubbels F, Jerome R, Vanlathem E, Deltour R, Blacher S and Brouers F 1998 Kinetic and thermodynamic control of the selective localization of carbon black at the interface of immiscible polymer blends *Chem. Mater.* **10** 1227–35

[37] Shahinpoor M and Kim K J 2000 The effect of surface-electrode resistance on the performance of ionic polymer–metal composite (IPMIC) artificial muscles *Smart Mater. Struct.* **9** 543–51

[38] Millet P, Andolfatto F and Durand R 1995 Preparation of solid polymer electrolyte composites-investigation of the precipitation process *J. Appl. Electrochem.* **25** 233–9

[39] Faez R, Gazotti W A and De Paoli M-A 1999 An elastomeric conductor based on polyaniline prepared by mechanical mixing *Polymer* **40** 5497–503

[40] Callister W D 2000 *Materials Science and Engineering: An Introduction* 5th edn (New York: Wiley)

[41] Ward I M and Hadley D W 1993 *An Introduction to the Mechanical Properties of Solid Polymers* (New York: Wiley)